in Aqueous Solution Over Copper Oxide," *Ind. Eng. Chem. Fundam.*, 13, 127 (1974).
Sano, Y., N. Yamaguchi, and T. Adachi, "Mass Transfer Coefficients for Suspended Particles in Agitated Vessels and Bubble Columns," *J. Chem. Eng. Japan*, 7, 255 (1974).
Satterfield, C. N., Y. H. Ma, and T. K. Sherwood, *The Effectiveness Factor in a Liquid-Filled Porous Catalyst*, Inst. Chem. Eng. Symp. Ser. No. 28, London (1968).
Satterfield, C. N., A. A. Pelossof, and T. K. Sherwood, "Mass Transfer Limitations in a Trickled-Bed Reactor," *AIChE J.*, 15, 226 (1969).
Satterfield, C. N., *Mass Transfer in Heterogeneous Catalysis*, MIT Press, Cambridge, Mass. (1970).
Satterfield, C. N., C. K. Colton, and W. H. Pitcher, Jr., "Restricted Diffusion in Liquids Within Fine Pores," *AIChE J.*, 19, 628 (1973).
Satterfield, C. N., "Trickle-Bed Reactors," *AIChE J.*, 21, 209 (1975).
Schlesinger, M. D., J. H. Crowell, M. Leva, and H. H. Storch, "Fischer-Tropsch Synthesis in Slurry Phase," *Ind. Eng. Chem.*, 43, 1474 (1951).
Shah, Y. T., G. Stiegel, and M. M. Sharma, "Backmixing in Gas-Liquid Reactors," *AIChE J.*, 24, 369 (1978).
Sherwood, T. K., and E. J. Farkas, "Studies of the Slurry Reactor," *Chem. Eng. Sci.*, 21, 573 (1966).
Shibuya, H., and Y. Uraguchi, "Effective Diffusivities in Activated Carbon Pellets by a Dynamic Wicke-Kallenbach Apparatus," *J. Chem. Eng., Japan*, 10, 446 (1977).
Shingu, H., "Oxidation of Ethylene to Ethylene Oxide Using Silver Catalyst," U.S. Patent 2,985,668 (May 23, 1961).
Slesser, C. G. M., W. T. Allen, A. R. Cumming, U. Pawlowshy, and J. Shields, "Study of Non-Catalytic Aspects of Catalyst Particle Influence in Slurried Bed Reactors," *Chem. Reaction Eng.*—Proc. Fourth European Sympos., Brussels, 41 (1968).
Suzuki, M., and K. Kawazoe, "Batch Measurement of Adsorption Rate in an Agitated Tank—Pore Diffusion Kinetics with Irreversible Isotherm," *J. Chem. Eng. Japan*, 7, 346 (1974).
Suzuki, M. and K. Kawazoe, "Effective Surface Diffusion Coefficients of Volatile Organics in Activated Carbon During Adsorption," *J. Chem. Eng., Japan*, 8, 379 (1975).
Sylvester, N. D., A. A. Kulkarni, and J. J. Carberry, "Slurry and Trickle Bed Reactor Effectiveness Factor," *Can. J. Chem. Eng.*, 53, 313 (1975).
Tamhankar, S. S., and R. V. Chaudhari, "Absorption and Reaction of Acetylene in Aqueous Cuprous Chloride Slurries," *Ind. Eng. Chem. Fundam.* 18, 406 (1979).
Tan, P. N., and J. S. Ratcliffe, "Catalytic Chlorination of Toluene in a Slurry Reactor," *Mech. Chem. Eng. Trans.*, MC 10, 35 (1974).
Tong, S. B., K. F. O'Driscoll, and G. L. Rempel, "Kinetics of Nitro Benzene Hydrogenation Using a Gel-entrapped Pd-Catalyst," *Can. J. Chem. Eng.*, 56, 340 (1978).
Tsuto, K., P. Harriott, and K. B. Bischoff, "Intraparticle Mass Transfer Effects and Selectivity in the Palladium-Catalyzed Hydrogenation of Methyl Linoleate," *Ind. Eng. Chem. Fundam.*, 17, 199 (1978).
van der Plank, P., Fifth European, Second Internat. Sympos. Chemical Reaction Engineering, Amsterdam (May 2-4, 1974).
Varghese, P., A. Varma, and J. J. Carberry, "Catalytic Effectiveness and Yield: The Case Involving Finite External and Internal Area," *Ind. Eng. Chem. Fundam.*, 17, 195 (1978).
Wei, J., "Intraparticle Diffusion Effects in Complex Systems of First Order Reactions," *J. Catalysis*, 1, 526 (1962).
Wilke, C. R., and P. Chang, "Correlation of Diffusion Coefficients in Dilute Solutions," *AIChE J.*, 1, 264 (1955).
Yagi, H., and F. Yoshida, "Gas Absorption by Newtonian and Non-Newtonian Fluids in Sparged Agitated Vessels," *Ind. Eng. Chem. Proc. Des. Dev.*, 14, 488 (1975).
Zwicky, J. J., and G. Gut, "Kinetics, Poisoning and Mass Transfer Effects in Liquid-Phase Hydrogenations of Phenolic Compounds Over a Palladium Catalyst," *Chem. Eng. Sci.*, 33, 1363 (1978).
Zweitering, T. N., "Suspending of Solid Particles in Liquid by Agitators," *Chem. Eng. Sci.*, 8, 244 (1958).

THE AUTHORS

Dr. R. V. Chaudhari obtained his PhD in chemistry from Bombay University. After spending a couple of years in University of Edinburgh, Scotland as a post-doctoral fellow, he joined the Chemical Engineering Division of National Chemical Laboratory, Poona, India as a scientist. Current areas of interest are gas-liquid reactions, three phase catalytic reactors and homogeneous catalysis. He has published over 20 papers in these areas.

Dr. P. A. Ramachandran has a PhD in chemical engineering from University of Bombay and has held teaching and post-doctoral positions in University of Bombay, India, University of Salford, UK, and University of California, Davis. His current position is as a scientist in the National Chemical Laboratory, Poona. He has published more than 50 papers in the areas of reaction engineering and mathematical modeling. Dr. Ramachandran is recipient of the "Moulton" medal (1971) from the Institution of Chemical Engineers, London.

Manuscript received February 26, 1979; revision received October 26, and accepted November 2, 1979.

Intraparticle Mass Transfer in Coal Pyrolysis

GEORGE R. GAVALAS

and

KARL A. WILKS

Division of Chemistry and Chemical Engineering
California Institute of Technology
Pasadena, California 91125

Intraparticle mass transfer in coal pyrolysis is described by ternary diffusion and viscous flow, in conjunction with a simple pore model to predict concentration profiles for gases and tar. At low pressures, product yields depend on particle size only, while at high pressures they depend on pressure and particle size. Limited experimental data from a subbituminous coal confirm these trends. Data from a bituminous coal show different trends, as expected from the drastic changes the pore structure undergoes during pyrolysis.

SCOPE

This study of intraparticle mass transfer in coal pyrolysis concentrates on the effect of pressure and particle size on the product yield. Three ingredients are required for a theoretical description of intraparticle transport: the chemistry of pyrolysis, a pore model of coal, and suitable flux relationships. The probability that a volatile product molecule recombines with the coal matrix before escaping the particle depends on the number of free radical sites

Wilks is now with Stauffer Chemical, Richmond, Calif.

on the condensed phase and on the rate of transport by diffusion and viscous flow. Once reattached, this molecule can again dissociate, unless additional bonds are produced by other reactions.

The details of such successive dissociation and recombination processes are at present poorly understood. Here, the detailed chemistry is bypassed by treating the net production of tar and gases as known quantities. The intraparticle concentrations of volatile species can then be calculated in a straightforward fashion, and the concentration of tar can be chosen as a measure of the effect of pore transfer on product yields. This relationship is only qualitative, and the theory is thereby limited to providing trends rather than quantitative results.

The pore model we use describes the continuous size distribution by a discrete one and, by means of connectivity arguments, elaborates the role of various pore sizes in mass transfer. In the case of pyrolysis, the lack of detailed chemical information suggests the selection of a relatively simple pore model. A two-pore-size model (0.1 μm, 1 μm) appears adequate, and under some conditions the 1 μm pores need not be considered in the flux relations, but only in determining an "effective" particle size.

The flux relations used are those of Mason and Evans (1969), including multicomponent diffusion and viscous flow in the transition regime. The various product species are lumped to a ternary system, gases, tar, and inert carrier. The resulting set of three ordinary differential equations for the concentration of gases, tar, and carrier is solved numerically.

Some experimental results concerning product yield from the pyrolysis of a subbituminous and a bituminous coal are reported. These and other results from the literature are compared with the predictions of the model.

CONCLUSIONS AND SIGNIFICANCE

Comparing pore-size distributions before and after pyrolysis indicates that subbituminous coals undergo some pore enlargement, but otherwise maintain a stable pore structure during pyrolysis. Coals that pass through a fluid stage (e.g., high-volatile bituminous) suffer more drastic changes, including collapse of pores in the range 0.002-0.008 μm and creation of bubbles. The mechanism of mass transfer in these two types of coal is evidently different, and our study is restricted to subbituminous coals that maintain a stable pore structure.

A simple pore model for a subbituminous coal is developed by representing the pore-size distribution curve with pores of five different diameters: micropores, 0.008, 0.1, 1 μm and 3 μm. The micropores are intimately connected with the intrinsic kinetics and are not considered in the analysis. The pores of 0.008 and 0.1 μm are the main carriers of reaction, while the pores of 0.1 and 1 μm are the main carriers of mass transport. At low temperature pyrolysis, the 1 μm pores can be taken into account by using an effective particle size. Mass transfer can then be described by the 0.1 μm pores alone. At higher temperatures, the high rates of pyrolysis induce significant concentration gradients in the 1 μm pores, and a two-pore-size model must be used.

Having selected a pore model, conservation equations are formulated by lumping the gaseous species into three generalized components: tar, gases (CO, CO_2, CH_4, etc.), and inert carrier (e.g., He), if present. We use the model of Mason and Evans (1969) to describe ternary diffusion, in the transition regime, and convective transfer (viscous flow) by pressure gradients. The resulting system of three ordinary differential equations is solved numerically to obtain the intraparticle concentration profiles of the three components: tar, gases and inert.

The average tar concentration is chosen as a suitable measure of transport limitations. Large tar concentration implies extensive recombination to the coal matrix, resulting in reduced weight loss and tar yield, and increased yield of gases. The main conclusions from the numerical results are: (a) at low pressures, the average tar concentration is independent of pressure but increases with particle size; (b) at high pressures, the average tar concentration increases with both pressure and particle size.

Pyrolysis experiments were performed with a subbituminous coal and an HVC bituminous coal. Although of limited accuracy, the results with the subbituminous coal show (in qualitative agreement with the model) that at low pressures ($10^4 - 2 \times 10^5$ N/m^2), the yield of gaseous products is independent of pressure, but increases with particle size. The same general result has been observed by others for the pyrolysis of lignite. Subbituminous coals and lignites maintain a relatively stable pore structure during pyrolysis. Coals which pass through a fluid stage during heating cannot be described by the model on account of the drastically changing pores structure and the possible role of bubbles in mass transfer. The results with the bituminous coal and other previously reported results are indeed at variance with the predictions of the model.

Pore diffusion and reaction have been studied extensively in the context of porous catalysts. The following brief review is limited to references that are relevant to coal pyrolysis either from the standpoint of diffusion alone or from the standpoint of diffusion and chemical reaction.

A general treatment of pore mass transfer must include the following factors: (a) multicomponent diffusion, (b) pressure gradients, and (c) diffusion in the transition regime for at least part of the porous structure. Jackson (1977) summarizes the theories that have been developed to account for these three factors. According to this monograph and some other recent papers, the dusty gas model and the related model of Feng and Stewart (1973) appear best suited to handle the general problem. Applying the dusty gas model requires the experimental determination of three parameters that characterize the porous medium, while the model of Feng and Stewart can, in principle, be applied given the pore-size distribution. In practice, however, this model also requires the

determination of a few adjustable parameters from diffusion data.

Analysis of combined diffusion and chemical reaction has followed two general approaches. In the first, the gaseous concentrations are taken to be the same in pores of different size located at the same macroscopic position within the particle. This "smooth field" assumption, as called by Jackson (1977), may be satisfactory for sufficiently high degree of pore crosslinking and relatively low reaction rates. The smooth field assumption allows the formulation of the reaction-diffusion problem using purely physical transport coefficients. In connection with the dusty gas model, this approach has given good agreement with experimental results in the work of Balder and Petersen (1968) and Wong and Denny (1974). Abed et al. (1973, 1974) used a similar approach in a theoretical study of effectiveness factors.

The second approach, which accounts for concentration differences between pores of different size, has been applied mainly in the context of the macropore-micropore model of Smith and coworkers: Wakao and Smith (1962, 1964), Rao and Smith (1964), Otani et al. (1965). In the experimental work of Rao and Smith, the micropore effectiveness factor was very close to unity, hence the smooth field approximation still applied. While early work with the micropore-macropore model has not used general flux relations, Jackson (1977) shows how these relationships can be applied to a macropore-micropore structure when the smooth field approximation is not adequate.

In contrast to the case of porous catalyst pellets, pore diffusion in coal or char particles has only recently been considered in kinetic studies. Arri and Amundson (1978) made a theoretical study of char gasification in which pore mass transfer was described by bulk diffusion using effective diffusivities. In an analysis of coal hydropyrolysis, Russel et al. (1978) described pore mass transfer by the dusty gas model assuming a single pore size, equal binary diffusivities and taking into account possible pressure build-up inside the particle. Although this study is limited to binary diffusion and does not take into account the distribution of pore sizes, it is the only existing study that considers the coupling between diffusional and viscous fluxes of volatiles in coal particles.

Compared to porous catalysts, coal has low porosity and broad pore size distribution. The largest pores, micron-sized, contribute substantially to purely physical transport but much less to coupled diffusion-reaction because of their low surface area and insignificant crosslinking. Hence, transport coefficients measured in the absence of reactions cannot be applied directly to describe diffusion and reaction. The role of pores of different sizes must be carefully assessed in each case, especially in the case of rapid processes such as pyrolysis and combustion.

THEORETICAL DEVELOPMENT

A Pore Model for Coal Particles

The pore volume distribution shown in Figure 1 is divided into five ranges, according to pore diameter. Range 1 consists of micropores 0.0004-0.0012 μm; range 2 of transitional pores 0.0012-0.03 μm; ranges 3, 4, and 5 consist of macropores 0.03-0.3 μm, 0.3-3 μm and 3-10 μm. The first range is defined by the molecular sieve properties of these pores. The others are defined largely arbitrarily, but such that the porosities $\epsilon_2, \ldots, \epsilon_5$ are of the same order of magnitude. Because of the rapidly declining pore volume distribution curve, each successive

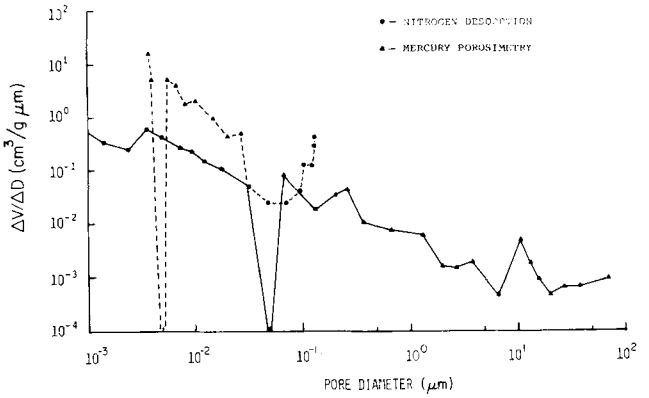

Figure 1. Pore volume distribution of a subbituminous coal (PSOC 241).

range has width which is an order of magnitude larger than the previous one.

Next, a representative or "average" diameter is assigned to each of the ranges 2-5. It is not necessary to assign a representative diameter to Range 1. These averages could be chosen on the basis of theoretical considerations or treated as adjustable parameters. In this analysis and many other problems, however, the results turn out not to be very sensitive to changes in the average diameters.

Having assigned average sizes, the continuous pore size distribution is replaced with a collection of pores of diameters $D_1, \ldots, D_5$ and pore volume fractions $\epsilon_1, \ldots, \epsilon_5$. The question that must be addressed next is that of *connectivity* or degree of crosslinking. The very broad pore size distribution and the low porosity make the assumption of "thorough crosslinking," implicit in the various catalyst pore models, not very suitable for fine particles of coal and char.

Consider a collection of pores of diameters, $D_1, \ldots, D_N$ and pore volume fractions $\epsilon_1, \ldots, \epsilon_N$. Characteristic lengths L_i, L'_i are defined for pores of diameter D_i such that L_i is the average pore length between intersections with pores of diameter D_i or larger, and L'_i is the average length between intersections with pores of diameter D_{i+1} or larger. Assuming that the pores are located in a random and isotropic fashion, the lengths L_i, L'_i are given by

$$\frac{1}{L_i} = \sum_{j=i}^{N} \frac{\epsilon_j}{D_j}\left(1 + \frac{D_i}{D_j}\right) \tag{1}$$

$$\frac{1}{L'_i} = \sum_{j=i+1}^{N} \frac{\epsilon_j}{D_j}\left(1 + \frac{D_i}{D_j}\right) = \frac{1}{L_{i+1}} \tag{2}$$

We also define by m_{ij} the number of intersections of D_i and D_j pores per unit particle volume and by n_i the number of pore-mouths of D_i-pores per unit particle external surface area. These quantities are given by

$$m_{ij} = \frac{4\epsilon_i\epsilon_j}{\pi D_i^2 D_j^2}(D_i + D_j) \tag{3}$$

$$n_i = \frac{2\epsilon_i}{\pi D_i^2} \tag{4}$$

The derivation of Equations (1)-(4) will be presented in a future report on coal combustion. Suffice it to note that when $N = 2$, the length L_2 must have the order of magnitude D_2/ϵ_2, simply by dimensional arguments. The significance of the quantities L_i, L'_i, m_i, n_{ij} will become clear in the next subsection.

Volatile Production and Mass Transfer in a Porous Coal Particle

The volatile products of pyrolysis fall into two general groups, gases and tar. The gases include H_2O, CO_2, CO and lower hydrocarbons, C_1-C_4. The tar consists of molecules which are produced with molecular weights in the range 250-450. Subsequent dimerization and association increases the molecular weight of the tar to the range 500-1,200 observed by vapor phase osmometry. See, for example, Gavalas and Oka (1978).

Although diffusion in Pore System 1, the micropores, is activated for both the gases and the tar, important differences exist between these two groups of compounds. At temperatures of 400-700°C, the gases are relatively unreactive and diffuse from Pore Range 1 to Pore Range 2 without reacting with the coal matrix. The tar molecules, on the other hand, are quite reactive. Initially produced as free radicals, they can readily recombine with free radical sites on the coal matrix. Even when these tar molecules are saturated by abstracting hydrogen from their surroundings, they may still react with free radical sites by means of addition reactions or be converted back to free radicals by losing hydrogen to the coal matrix. Because of their relatively large size, the tar molecules diffuse extremely slowly through the micropores. Thus, the probability that a tar molecule escapes to the gas phase is extremely small, unless it is generated near the surface of D_2 or larger pores. Since this surface is distributed throughout the coal particle, tar production reaction appears to be volumetric.

As tar molecules are removed from the surface of D_2-pores, other molecules become accessible and the reaction proceeds by what is akin to a shell-progressive mechanism. Tar molecules inaccessible to the pores of Range 2 or higher, participate in reactions which produce gas and cause further crosslinking. The tar and gas molecules released from the surface of D_2-pores are carried through these pores to D_3, D_4 and D_5 pores. During transport through the D_2-pores, the tar molecules are subject to recombination with surface sites of the coal matrix. Once in pores of Range 3 of higher, the loss by recombination becomes much less important, because of the small surface area associated with the larger pores.

To evaluate the role of the pores D_2, D_3, D_4, and D_5 in mass transfer, we examined the magnitude of the quantities L_i, L'_i, n_i, m_{ij}. Taking as an example the pore volume distribution of Figure 1, we have $\epsilon_2 = 0.005$, $\epsilon_3 = 0.01$, $\epsilon_4 = 0.015$, $\epsilon_5 = 0.019$. The values of the average diameters D_2, D_3, D_4, D_5 are chosen as 0.008, 0.1, 1, 6 μm, respectively. Using Equations (1)-(4) we compute

$$L_2 = 0.74\ \mu\text{m}, \quad L'_2 = L_3 = 4.6\ \mu\text{m},$$

$$L'_3 = L_4 = 29.7\ \mu\text{m}, \quad L'_4 = L_5 = 158\ \mu\text{m}$$

$$m_{23} = 10.7/(\mu\text{m})^3, \quad m_{24} = 1.5/(\mu\text{m})^3,$$

$$m_{25} = 0.315/(\mu\text{m})^3$$

$$m_{34} = 0.021/(\mu\text{m})^3, \quad m_{35} = 0.004/(\mu\text{m})^3$$

$$n_2 = 49.7/(\mu\text{m})^2, \quad n_3 = 0.64/(\mu\text{m})^2, \quad n_4 = 0.01/(\mu\text{m})^2$$

We note first that the D_2-pores contain most of the active surface area for product generation and recombination. This pore range makes a relatively small contribution to mass transfer because of low permeability and Knudsen diffusivity, although the porosity is comparable to that of the other ranges. On the other hand, a comparison between L'_2 and D_p indicates that the D_2-pores are relatively well crosslinked with the larger pores. Hence, the products generated in the D_2-pores are transported to the outside via the larger pores rather than directly. The latter conclusion also follows by computing the ratio of pore-pore to pore-external surface intersections,

$$\frac{(m_{23} + m_{24} + m_{25})\pi D_p^3/6}{n_2 \pi D_p^2}$$

For a 100 μm particle, this ratio is equal to 4.1, indicating that most of the D_2-pore mouths are found on larger pores rather than on the surface of the particle. On the basis of these considerations, the D_2-pores will be treated as source terms for the larger pores while their contribution to transport will be neglected.

Next, the D_3-pores are considered. The values $L_3 = 4.6\ \mu$m, $L'_3 = 29.7\ \mu$m indicate that these pores are well connected with each other but rather poorly with larger pores. Moreover, the ratio

$$\frac{(m_{34} + m_{35})\pi D_p^3/6}{n_3 \pi D_p^2}$$

is equal to 0.64 (for $D_p = 100\ \mu$m), indicating that the transport of products through the D_3-pores occurs partly directly to the particle surface and partly via the D_4-pores. Thus, the D_3- and D_4-pores must be considered interactively. But the magnitude $L_4 = 29.7$ indicates that the D_4-pores are not well connected with each other. Therefore, the use of an effective diffusivity incorporating the combined effect of D_3 and D_4 pores is questionable. Before proposing an alternate analysis of the transport problem, we note that the D_5-pores make a minor contribution to transport since $m_{25} << m_{23}, m_{24}$; $m_{35} << m_{34}$. These pores will be neglected from now on.

The transport in a two-sized pore system (D_3 and D_4) wherein the D_4-pores are not well crosslinked is an intriguing but unsolved problem. Nevertheless, in the limiting case when the pressure and composition gradients in the D_4-pores are negligible, a nonrigorous but physically appealing solution can be found. When the gas in the D_4-pores is at the same conditions as at the external particle surface, the D_4-pores essentially act to decrease the effective particle size such that

$$\frac{n_3 \pi D_{pe}^2}{\pi D_{p3}^3/6} = \frac{n_3 \pi D_p^2 + m_{34}\pi D_p^2/6}{\pi D_p^2/6}$$

In other words, we define a fictitious particle of diameter D_{pe} having only D_3-pores such that the number of D_3-pore mouths (lying on the external surface) per unit volume of the fictitious particle is equal to the number of D_3-pore mouths (lying on external surface and on D_4-pores) in the real particle. This equation defines the effective diameter D_{pe},

$$\frac{1}{D_{pe}} = \frac{1}{D_p} + \frac{m_{34}}{6n_3} \tag{5}$$

With the previous values ($D_p = 100\ \mu$m), we obtain $D_{pe} = 64.6\ \mu$m. The range of validity of the assumption of no concentration gradients in the D_4-pores is examined in Appendix A.

In view of the above discussion, it will be assumed that the reaction products are carried exclusively by the D_3-pores, while the D_2-pores act as reaction sources or sinks and the D_4-pores act to reduce the effective particle size.

The mass transfer problem is further simplified by lumping the various gaseous components into two or

three groups: the carrier gas (I), the permanent gases produced in pyrolysis (G), and the tar (T). This distinction is made on the basis of the magnitude of the Knudsen and molecular diffusion coefficients of these three groups. The diffusion coefficients of the tar molecules are the smallest, mainly because of the large molecular weight. The distinction between the carrier gas (I) and the other gases (G) is important when the former is helium or hydrogen as in many experimental studies. When the carrier gas consists of pyrolysis gases CO, CO_2, etc., as in some commercial processes, no distinction is necessary.

Certain additional assumptions are introduced before the problem is formulated quantitatively. First, the particle is considered as isothermal. The validity of this assumption depends on a number of factors, chiefly particle size and temperature of pyrolysis. For particles up to 500 μm and pyrolysis temperatures up to 600°C the temperature variation within the particle is not expected to exceed a few degrees centigrade. Under isothermal conditions, the net rate of formation of various gases and tar by pyrolysis is assumed to be independent of radial position within the coal particle. This is a good assumption when the effect of mass transfer is relatively small; otherwise, tar recombination would be more extensive near the center of the particle producing radial variations in the composition of the solid coal. Clearly such effects cannot be described without a detailed knowledge of the chemistry of pyrolysis. Finally, it is assumed that the characteristic time for mass transfer is much shorter than that for pyrolysis; therefore we need only consider the steady state mass transfer problem. The assumptions of isothermal particles and pseudo-steady-state mass transfer have been discussed by Russel et al. (1979). When the conditions for using an effective particle size are satisfied (see Appendix), the particles are essentially isothermal.

Pyrolysis with Ternary Mass Transfer

The mass balances for the three components, gases (G), tar (T), and carrier (I) in a spherical coal particle are

$$\frac{1}{r^2}\frac{d}{dr}(r^2N_G) = \gamma_G \tag{6}$$

$$\frac{1}{r^2}\frac{d}{dr}(r^2N_T) = \gamma_T \tag{7}$$

$$\frac{1}{r^2}\frac{d}{dr}(r^2N_I) = 0 \tag{8}$$

where the molar fluxes N_G, N_T, and N_I are based on total cross-sectional area. The quantities γ_G and γ_T are source terms due to pyrolysis in moles per unit total volume and time. The quantity γ_T is the net production rate of tar (i.e., the difference between forward and reverse rates and as such it includes the effect of diffusion and reaction in pore system 2). In this analysis, the terms γ_T, and γ_G, are regarded as quantities known from experiments. Assuming that γ_T and γ_G are independent of radial position, Equations (6)-(8) can be integrated to obtain

$$N_G = \gamma_G\frac{r}{3}, \quad N_T = \gamma_T\frac{r}{3}, \quad N_I = 0 \tag{9}$$

As discussed previously, the pressure and composition gradients need to be considered only in the D_3-pore network. For pores of uniform size and random isotropic orientation, we can use Feng and Stewart's (1973) adaptation of the Mason and Evans (1969) flux model, namely

$$N_i = -c_i\frac{\beta}{\mu}\frac{dP}{dr} + N_i' \quad (i = G, T, I) \tag{10}$$

where the permeability β is given by

$$\beta = \frac{D_3^2}{96}\epsilon_3$$

The diffusive fluxes N_i' satisfy the equations

$$\frac{dC_G}{dr} = -\frac{N_G'}{D_{GK}} + \frac{N_T'x_G - N_G'x_T}{D_{GT}} + \frac{N_I'x_G - N_G'x_I}{D_{GI}} \tag{11}$$

$$\frac{dC_T}{dr} = -\frac{N_T'}{D_{TK}} + \frac{N_G'x_T - N_T'x_G}{D_{GT}} + \frac{N_I'x_T - N_T'x_I}{D_{TI}} \tag{12}$$

$$\frac{dC_I}{dr} = -\frac{N_I'}{D_{IK}} + \frac{N_G'x_I - N_I'x_G}{D_{GI}} + \frac{N_T'x_I - N_I'x_T}{D_{TI}} \tag{13}$$

Here D_{iK} and D_{ij} ($i, j = G, T, I$) are effective Knudsen and binary (bulk) diffusion coefficients given by

$$D_{iK} = \frac{\epsilon_3}{3}D_{iK}^* \tag{14}$$

where

$$D_{iK}^* = 4.85 \times 10^3(T/M_i)^{1/2}D_3 \tag{15}$$

and all lengths are in cm.

$$D_{ij} = \frac{P_{at}}{P}\frac{\epsilon_3}{3}D_{ij}^{at} \tag{16}$$

where D_{ij}^{at} are the binary diffusion coefficients at $P_{at}(= 1\ at)$. Equations (10)-(13) describe mass transfer in the transition regime and reduce to the Knudsen and bulk regimes at the limit of low and large pressures. The three effective transport parameters β, D_{ik}, D_{ij} include a tortuosity factor of 3, corresponding to an isotropic pore system. Larger tortuosities can be used to account for deviation of the pores from the idealized cylindrical shape.

Equations (9) and (10) provide expressions for the diffusive fluxes N_i'

$$N_G' = \frac{\gamma_G r}{3} + C_G\frac{\beta}{\mu}\frac{dP}{dr} \tag{17}$$

$$N_T' = \frac{\gamma_T r}{3} + C_T\frac{\beta}{\mu}\frac{dP}{dr} \tag{18}$$

$$N_I' = C_I\frac{\beta}{\mu}\frac{dP}{dr} \tag{19}$$

which can be introduced into Equations (11)-(13) to eliminate N_i',

$$\frac{dC_G}{dr} = -\frac{\beta}{\mu}\frac{C_G}{D_{GK}}\frac{dP}{dr} - \frac{r}{3}\left[\gamma_G\left(\frac{x_I}{D_{GI}} + \frac{x_T}{D_{GT}} + \frac{1}{D_{GK}}\right) - \gamma_T\frac{x_G}{D_{GT}}\right] \tag{20}$$

$$\frac{dC_T}{dr} = -\frac{\beta}{\mu}\frac{C_T}{D_{TK}}\frac{dP}{dr}$$

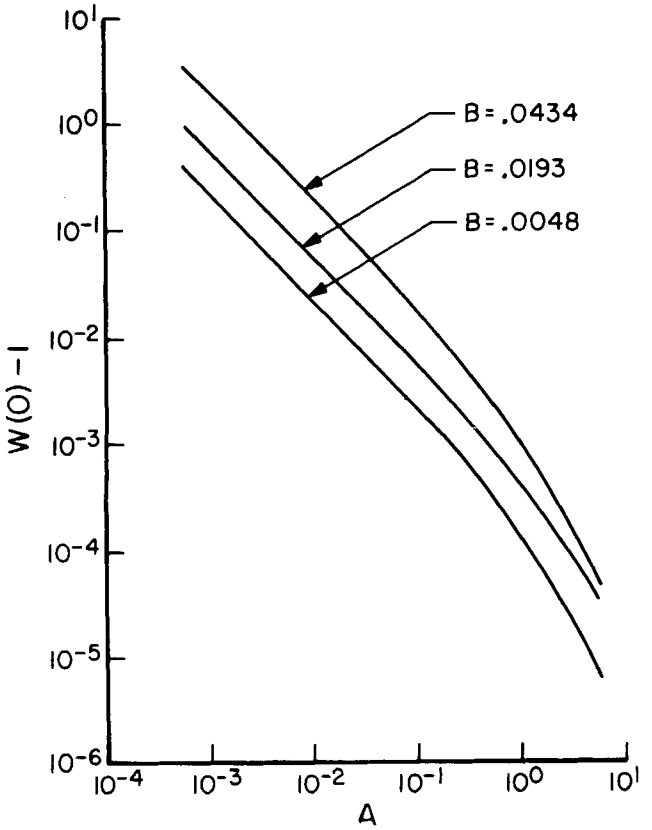

Figure 2. Dimensionless pressure build-up as a function of parameters *A*, *B*.

$$-\frac{r}{3}\left[\gamma_T\left(\frac{x_I}{D_{TI}}+\frac{x_G}{D_{GT}}+\frac{1}{D_{TK}}\right)-\gamma_G\frac{x_T}{D_{GT}}\right] \quad (21)$$

$$\frac{dC_I}{dr}=-\frac{\beta}{\mu}\frac{C_I}{D_{IK}}\frac{dP}{dr}+\frac{r}{3}\left(\frac{\gamma_G}{D_{GI}}+\frac{\gamma_T}{D_{TI}}\right)x_I \quad (22)$$

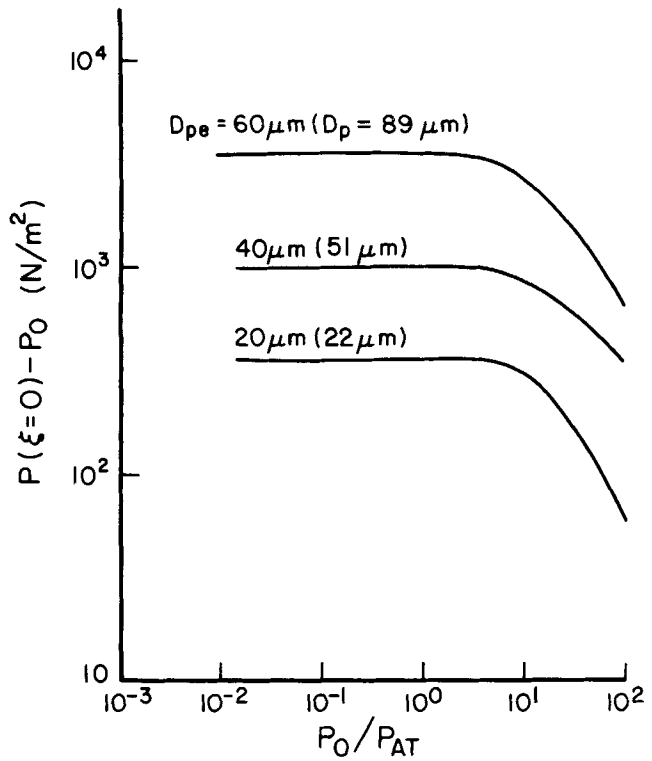

Figure 3. Effect of pressure and particle size on intraparticle pressure build-up.

By adding the above three equations, there is obtained

$$\frac{dP}{dr}=-\frac{R_gT\left(\frac{\gamma_G}{D_{GK}}+\frac{\gamma_T}{D_{TK}}\right)}{1+\frac{\beta}{\mu}P\left(\frac{x_G}{D_{GK}}+\frac{x_T}{D_{TK}}+\frac{x_I}{D_{IK}}\right)}\frac{r}{3} \quad (23)$$

This equation can be inserted in Equations (20)-(22) to eliminate dP/dr and obtain, in dimensionless form,

$$\frac{dV_G}{d\xi}=B\xi\Big[F\,V_G-\left(\frac{P_{at}}{P_o}+\lambda_{GI}V_I+\lambda_{GT}V_T\right)+\delta\lambda_{GT}V_G\Big] \quad (24)$$

$$\frac{dV_T}{d\xi}=B\xi\Big[F\,\rho_T\,V_T-\delta\left(\rho_T\frac{P_{at}}{P_o}+\lambda_{TI}V_I+\lambda_{GT}V_G\right)+\lambda_{GT}V_T\Big] \quad (25)$$

$$\frac{dV_I}{d\xi}=B\xi\left[F\,\rho_I\,V_I+(\lambda_{GI}+\delta\lambda_{TI})\,V_I\right] \quad (26)$$

$$\xi=1:\quad V_G=x_{Go},\quad V_T=x_{To},\quad V_I=x_{Io} \quad (27)$$

where

$$\xi=\frac{r}{R_p}$$

$$V_i=\frac{C_iR_GT}{P_o}\quad(i=G,T,I)$$

$$\rho_T=\frac{D^*_{GK}}{D^*_{TK}},\quad \rho_I=\frac{D^*_{GK}}{D^*_{IK}}$$

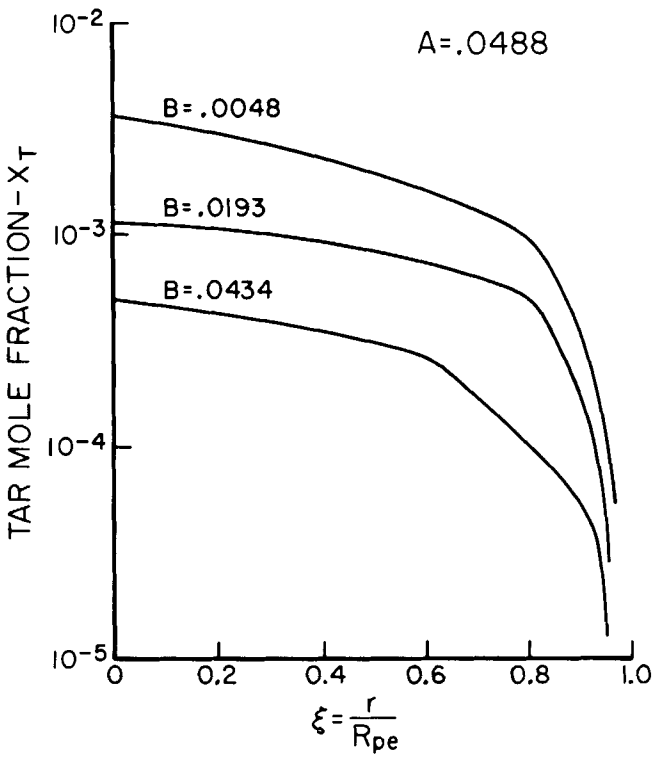

Figure 4. Tar mole fraction as a function of intraparticle position.

$$\lambda_{ij} = \frac{D^*_{GK}}{D^{at}_{ij}} \quad (i,j = T,I)$$

$$\delta = \frac{\gamma_T}{\gamma_G}$$

$$A = \frac{3\beta P_o}{\epsilon_3 \mu D^*_{GK}}$$

$$B = \frac{R_g T R_p^2 \gamma_G}{\epsilon_3 P_{at} D^*_{GK}}$$

$$F = \frac{(1+\delta\rho_T)A}{1+(V_G+\rho_T V_T+\rho_I V_I)A}\frac{P_{at}}{P_o}$$

The dimensionless pressure $W = P/P_o = V_G + V_T + V_I$ satisfies the equation obtained by adding (24)-(26)

$$\frac{dW}{d\xi} = -\frac{P_{at}}{P_o}\frac{1+\delta\rho_T}{1+A(V_G+\rho_T V_T+\rho_I V_I)}B\xi \tag{28}$$

$$\xi = 1:\ W = 1 \tag{29}$$

Although linearly dependent on Equations (24)-(27), Equation (28) is useful in certain limiting cases where it can be solved independently.

Among the dimensionless parameters appearing in Equations (24)-(28), only A and B need interpretation. For a given coal, A essentially depends on pressure only and represents the ratio of characteristic times for diffusion and forced flow (due to the pressure gradient). Large values of A indicate that the dominant transport mechanism is forced flow while small values signify the dominance of diffusion. Parameter B is a ratio of characteristic times for diffusion and reaction and encompasses the effect of particle size and rate of pyrolysis. At atmospheric or lower pressures, when A is small and transport occurs mainly by diffusion, the concentration profiles of the pyrolysis products are determined by the parameter B alone.

Russel et al. (1979) developed a model for coal hydropyrolysis which used the same flux relations as Equations (10)-(14), except that diffusion was assumed to be in the bulk regime, (on account of the high pressure), and all binary diffusion coefficients were set equal to each other. Effective diffusivity and permeability were used, and questions of pore connectivity were not considered. In the balance equations used by these authors, the reaction rate terms were functions of the dependent variables, and the formulation resulted in a boundary value problem. The present case is simpler, for the treatment of the reaction rates as known quantities allows the integration leading to Equation (9), resulting in an initial value problem. It may further be pointed out that the dimensionless parameters B and B/A are closely related, but not identical, to the parameters α^2 and ϵ of Russel, et al.

Equations (21)-(24) were solved numerically for various pressures P_o and particle sizes D_p. The transport coefficients were chosen on the basis of I:He, G:CO_2, and T: a compound having molecular weight 400 and binary coefficients $D^{at}_{TI} = 1.2$ cm²/s, $D^{at}_{TG} = 0.37$ cm²/s, all at 500°C. Calculations were made with $D_3 = 0.075$, 0.1, 1.5 μm to test the effect of the choice of the average radius of pores in Range 3. The surface conditions were $x_{Io} = 0.5$, $x_{Go} = 0.5$, $x_{To} = 0$.

Figure 2 shows the dimensionless intraparticle pressure build-up, as a function of the dimensionless parameters A and B. At low values of A, the dimensionless pressure buildup increases rapidly with B and decreases linearly with A. This behavior is more clearly discussed in terms of dimensional variables in Figure 3. At low values of the outside pressure P_o, the pressure buildup increases rapidly with particle size and is essentially independent of P_o. At higher values of P_o, the pressure buildup decreases with increasing P_o.

Figure 4 shows the mole fraction of tar as a function of reduced position, while Figure 5 shows the tar concentration averaged over the volume of the particle as a function of A and B. At low values of A, this concentration increases with B and is independent of A. At high values of A, the tar concentration increases rapidly with both A and B. To interpret these trends dimensionally, we recall that A essentially depends on the pressure only, while B depends on the particle size and the temperature which determines the rates γ_G, γ_T. At low pressures, the tar concentration increases with particle size or temperature but is independent of pressure. At higher pressures, the tar concentration increases with particle size, temperature and pressure. When the temperature is fixed, the effect of particle size and pressure is obvious, since increased tar concentration implies increased recombination and other secondary reactions resulting in higher gas and lower tar yields.

Whether the above effects of particle size and pressure are attenuated or accentuated with increasing temperature is unclear. Apart from its modest effect on transport coefficients and the previously mentioned effect on the tar concentration, via the parameter B, the temperature controls the rates of recombination and other secondary reactions and the duration of the overall process. The results of these individual influences cannot be determined without considering the chemical processes in some detail.

An important parameter in the model is the average diameter D_3 chosen to represent the pores in Range 3 (0.03-0.3 μm). The shape of the pore distribution in that range (Figure 1) suggests that D_3 should be about 0.07 to 0.15 μm. The results in Figures 2-5 were all obtained with $D_3 = 0.1$ μm. To test the sensitivity of the results to the value of D_3, additional calculations were performed with $D_3 = 0.075$ and 0.15 μm. As shown in Figure 6, the effect of D_3 is modest. For example, at atmospheric pressure the average tar concentration takes the values 5.68×10^{-10}, 4.37×10^{-10} and 3.07×10^{-10} moles/cm³ for $D_3 = 0.075$, 0.1 and 0.15 μm, respectively.

Special Case: Binary Mass Transfer

When the coal particles are surrounded by the pyrolysis gases alone, without any additional carrier gas, the problem essentially reduces to binary mass transfer. The pertinent equations are obtained by setting $V_I = 0$ in Equations (21)-(25).

$$\frac{dV_G}{d\xi} = B\xi\left(F_1 V_G - \frac{P_{at}}{P_o} - \lambda_{GT}V_T + \delta\lambda_{GT}V_G\right) \tag{30}$$

$$\frac{dV_T}{d\xi} = B\xi\left(F_1\rho_T V_T - \delta\rho_T\frac{P_{at}}{P_o} - \delta\lambda_{GT}V_G + \lambda_{GT}V_T\right) \tag{31}$$

$$\xi = 1:\quad V_G = x_{Go},\quad V_T = x_{To},\quad x_{Go} + x_{To} = 1 \tag{32}$$

$$\frac{dW}{d\xi} = -\frac{P_{at}}{P_o}\frac{1+\delta\rho_T}{1+A(V_G+\rho_T V_T)}B\xi \tag{33}$$

Table 1. Elemental Analysis (Ultimate, Dry) for Different Particle Sizes of the HVC Bituminous and Subbituminous B Coals

	HVC Bituminous		Subbituminous B	
	$\overline{D_p}$ (μm)		$\overline{D_p}$ (μm)	
	110	450	110	450
% ash	8.1	6.9	8.8	6.0
% C	72.9	73.8	65.6	67.8
% H	5.0	5.2	4.5	4.7
% N	1.4	1.5	1.2	1.2
%S	3.3	3.0	1.2	0.8
% O (by diff.)	9.3	9.6	18.7	19.5

where

$$F_1 = \frac{(1+\delta\rho_T)A}{1+(V_G+\rho_T V_T)A}\frac{P_{at}}{P_o} \tag{34}$$

Equations (30)-(32) were solved numerically for surface conditions $x_{Go} = 1$, $x_{To} = 0$. The results obtained were practically identical to the results of Figures 2-4 (which correspond to $x_{Go} = 0.5$, $x_{To} = 0$, $x_{Io} = 0.5$) as far as pressure build-up and average concentration of tar are concerned. These results suggest that the presence of helium or any other inert carrier does not have a significant effect on intraparticle tar transport.

Although the numerical solution of Equations (30)-(33) provides all required information concerning tar transport, it is interesting to obtain some analytical results concerning pressure build-up from a simplified version of Equation (33). In the pyrolysis of subbituminous coals, the yield of gaseous products usually exceeds the yield of tar on a mass basis. Hence, on a molar basis, $\gamma_T << \gamma_G$, i.e., $\delta << 1$. If, in addition $x_{To} << 1$, $V_T/V_G << 1$ the approximations

$$V_G + \rho_T V_T \simeq V_G, \quad W \simeq V_G \tag{35}$$

can be used to simplify Equation (33) to

$$\frac{dW}{d\xi} = -\frac{P_{at}}{P_o}\frac{1+\delta\rho_T}{1+Aw}B\xi \tag{36}$$

which can be integrated immediately. The maximum pressure at the center is then given by

$$W(0) - 1 = -\frac{1+A}{A}\left\{\left(1+\frac{A_{at}(1+\delta\rho_T)B}{(1+A)^2}\right)^{1/2} - 1\right\} \tag{37}$$

where

$$A_{at} = \frac{3\beta P_{at}}{\epsilon_3\mu D_{GK}^{\bullet}} \tag{38}$$

Under all conditions of interest $A_{at} << 1$ so that as long as B is not much larger than one, (37) can be simplified to

$$W(0) - 1 = \frac{1+\delta\rho_T}{2}\frac{A_{at}}{A(1+A)}B \tag{39}$$

The relative pressure build-up is proportional to B which incorporates the effect of particle size and rate of pyrolysis (which depends on temperature). The outside pressure has an effect through the factor $A(1+A)$. At low outside pressures ($P_o << P_{at}$), the relative pressure increase is large while at large pressures the relative pressure increase is small.

EXPERIMENTAL

Coal Samples

Pyrolysis experiments were performed with two different coals, a high volatile C bituminous, Kentucky No. 9, and a subbituminous B, PSOC 241, obtained from the Pennsylvania

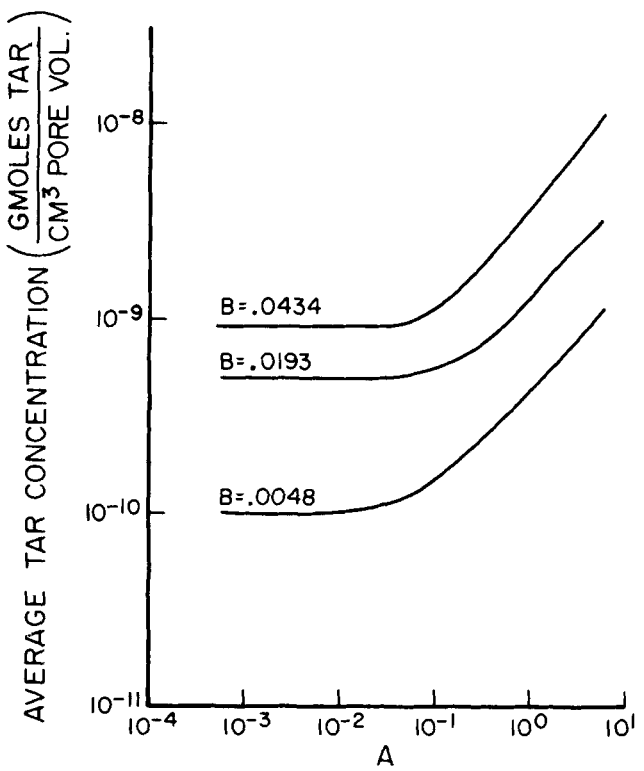

Figure 5. Average intraparticle tar concentration as a function of parameters A, B.

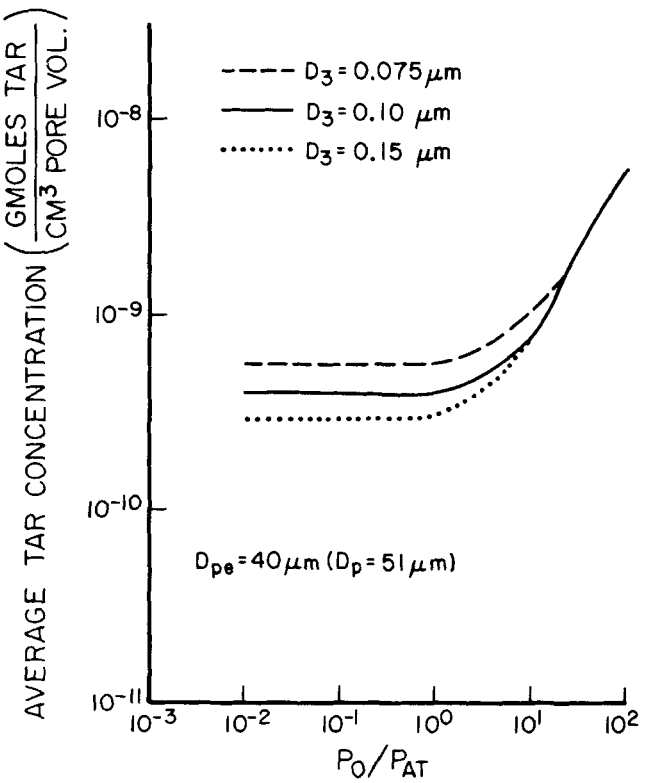

Figure 6. Effect of D_3-pore diameter on the average intraparticle tar concentration.

State University. The coals were crushed and seived into two particle-size fractions (−35 to +45 and −120 to +170 U.S. mesh). Drying took place under vacuum at 100°C, and the dry, ultimate analyses for these fractions are shown in Table 1. Pore volume and pore area distributions were calculated from nitrogen adsorption isotherms performed by Pacific Sorption Service and mercury porosimetry performed by the Micromeritics Instrument Corporation.

Pyrolysis Experiments

The coal samples were pyrolyzed by placing 200 mg. samples in a folded, resistance-heated, 325 mesh stainless-steel screen. A power supply (100 A maximum output) regulated by a control circuit provided two-stage current pulses which generated initial heating rates of approximately 600°C/s and maintained steady state temperatures as high as 1000°C, indefinitely. The temperature was measured by a 3 mil thermocouple placed inside the folds of the screen. The pressure in the reactor was varied between 10^4 and 2×10^5 N/m^2, and all pyrolysis reactions were carried out using helium as an inert carrier. Gaseous products were sampled directly from the 1300 cm^3 reaction vessel and analyzed by gas chromatography. The heavy products condensed on aluminum foils lining the walls of the reactor, which were removed and weighed. The remaining char was also collected and weighed after gas analysis.

Gas Chromatography

Hydrocarbon gases were analyzed on a Hewlett-Packard Hp 5710 A gas chromatograph equipped with a flame ionization detector. A 2m by 3 mm stainless steel column packed with 80/100 mesh Porapak T was used in a temperature programming sequence from 50 to 140°C @ 0.67 °C/s. Nitrogen was used as the carrier gas, and C_1 through C_6 hydrocarbons were detected. Carbon oxides and water were analyzed using Varian Aerograph Series 1400, thermal conductivity detector. The gas separation was accomplished by passing helium through a 3 m by 3 mm s.s. column packed with 120/140 mesh Carboseive B coupled with a 0.3 m by 3 mm s.s. column of 80/100 mesh Porapak T. The column was held isothermally for 180 seconds and then temperature programmed from 35 to 140°C at 0.17 °C/s. Data reduction was accomplished using a Spectra-Physics, Autolab computing integrator.

RESULTS AND DISCUSSION

Physical Characteristics

To observe the transport of volatiles in coal, pyrolysis experiments were performed on two different particle-size fractions. As seen in Table 1, the elemental compositions for the smaller particle size of each coal was slightly different, due to ash enrichment of the sample during the sieving process. But, the ash-free contents of carbon and hydrogen are virtually identical.

In addition to elemental analyses, pore area and pore volume were measured on the two coals before and after pyrolysis. Because the subbituminous *B* coal is of particular interest from a modeling viewpoint, additional pore volume information was obtained by mercury porosimetry.

Figure 1 combines the nitrogen adsorption and mercury porosimetry data for this coal to show its pore volume distribution over the complete pore size range from micro- to macro-pores. Although there is considerable discrepancy between the nitrogen and mercury data* in their region of overlap, 0.03 μm was taken as the boundary separating the range of greatest accuracy of each measurement. Below 0.03 μm, more emphasis is placed on the validity of the nitrogen pore volume distribution. Above that, the mercury porosimetry data is considered more representative.

* Lack of agreement between the two methods is attributed to the extreme complexity of the pore structure of coal.

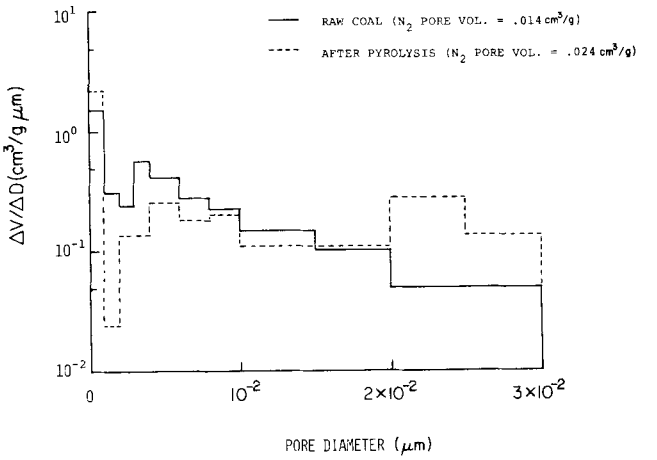

Figure 7. Pore volume distribution of PSOC 241 before and after pyrolysis.

The pore area and pore volume of the subbituminous *B* coal were measured before and after pyrolysis in helium at 500°C and atmospheric pressure using nitrogen adsorption, Figure 7. The pyrolysis resulted in an increase of pores above 0.015 μm and an elimination of pores below that size. But, the coal does appear to retain its general pore structure. The pore area is 2.20 m^2/g for the raw coal and 2.16 m^2/g for the pyrolyzed coal.

The pore volume distribution for the mildly swelling, HVC bituminous coal showed considerable change after pyrolysis, (Figure 8). Much of the micropore structure was altered by complete elimination of pores in the range of 0.002 to 0.006 m, but the total pore volume increased. The pore area distribution followed the same pattern as the pore volume distribution with the area increasing from 4.20 m^2/g before to 6.31 m^2/g after pyrolysis. Carbon dioxide surface areas for the same samples also increased from 147 m^2/g before to 170 m^2/g after pyrolysis.

Pyrolysis Yields

Two particle sizes of the subbituminous B and HVC bituminous coals were pyrolyzed at 500°C at various pressures. The overall weight loss of these coals showed no effect of particle size. At 500°C and 10^4 N/m^2 helium, the subbituminous B coal lost 19% of its weight, while the HVC coal experienced a 26% weight loss. There was

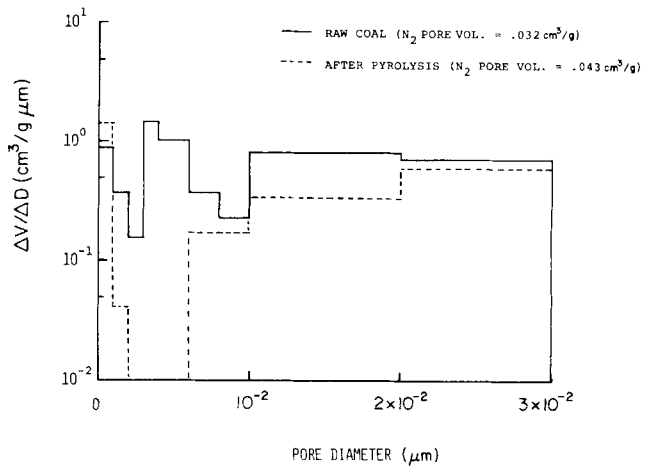

Figure 8. Pore volume distribution of Kentucky #9 before and after pyrolysis.

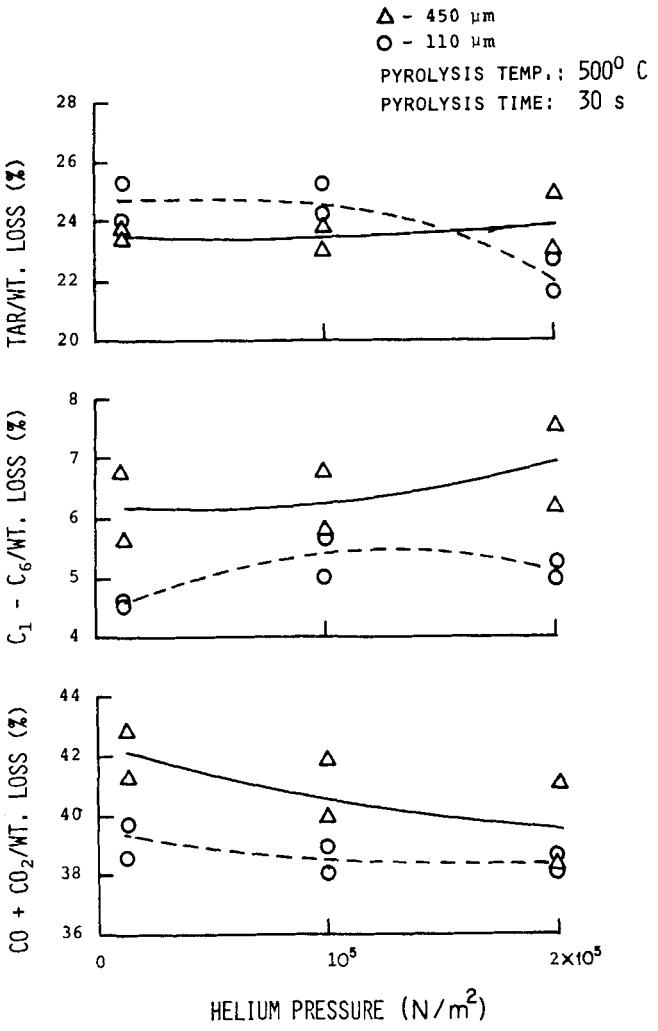

Figure 9. Effect of pressure and particle size on relative yields of pyrolysis products from PSOC 241.

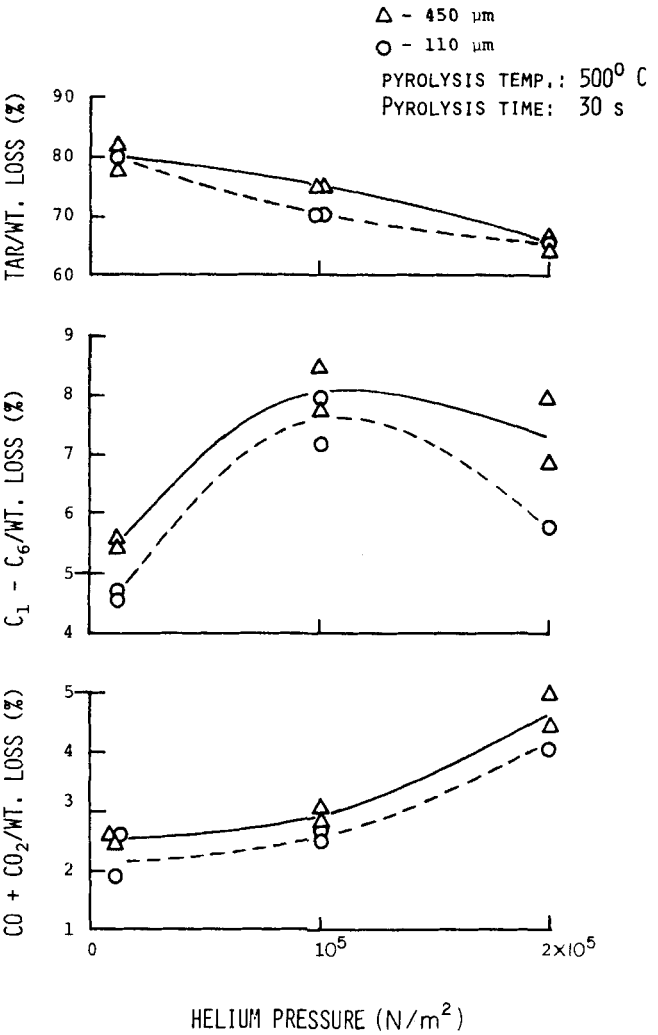

Figure 10. Effect of pressure and particle size on relative yields of pyrolysis products from Kentucky #9.

a slight variation in weight loss with pressure for the subbituminous B coal. This was mainly attributed to variations in sample temperature (an effect of pressure changing the rate of heat transfer around the sample screen and thus affecting sample temperature). But the HVC bituminous coal did decrease in weight with increased helium pressure. The weight loss decreased from 26 to 19% when the helium pressure was raised from 10^4 to 2×10^5 N/m^2.

The effect of particle size and pressure is best studied from plots of relative yield, in which variations due to small uncontrolled temperature changes are suppressed. Figures 9 and 10 show the yield of products from the subbituminous and the bituminous coals plotted versus helium pressure. The difference between the distribution of types of products for these two coals is considerable. The subbituminous B coal produces much less tar and considerably more carbon oxides. There is also a large difference in the amount of water produced. Approximate yields of water determined by gas chromatography were 32% of weight loss for the subbituminous coal, compared to 9.6% for the HVC bituminous coal.

Considering first the results for the subbituminous coal, we note the yield increase of carbon oxides and C_1 through C_6 hydrocarbons with increased particle size. This is due to stripping of side chains from tar molecules, which participate in more extensive dissociation and recombination reactions before ultimate release or conversion to char. This interpretation is compatible to the transport model developed earlier which, as shown in Figure 5, predicted that the pseudo-steady-state intraparticle tar concentration increases with particle size at fixed total pressure. The increased yield of gases should be accompanied by a corresponding decrease in the yield of tar. However, the tar collection procedure was not sufficiently accurate to clearly show this effect.

Product yields of the subbituminous coal showed no significant effect of pressure in the range 10^4 to 2×10^5 N/m^2. Any variations (shown in Figure 9) with respect to pressure are probably due to experimental error. Suuberg et al. (1978) observed no difference in product yields from the pyrolysis of lignite between vacuum and one atmosphere pressure up to temperatures of 800°C. These results agree with those of Figure 5, showing that at low pressures, the effect of pressure on tar concentration is negligible. At 850 to 1,000°C, Suuberg (1977) found significantly lower tar yield in the pyrolysis of lignite in helium when the pressure was increased from 10^5 to 7×10^6 N/m^2. Unfortunately, these temperatures are too high for meaningful comparison with the present model.

The experimental results with the high volatile bituminous coal (Figure 10) show a slight increase of carbon oxides and hydrocarbons and decreased tar, with increasing particle size and increasing pressure. The decreased weight loss and yield of tar and the increase in gas yield

due to increased pressure were observed in the results of Anthony et al. (1976) and Suuberg (1977) over a wide pressure range. The transport model of the previous section is not directly applicable in interpreting these results and, in fact, the observed pressure effects in the low-pressure region, vacuum to two atmospheres, are at variance with the predictions of Figure 6.

ACKNOWLEDGMENT

This work was supported by the National Science Foundation under Grant No. AER 74-12161.

NOTATION

A = dimensionless parameter
$\overline{A}$ = dimensionless parameter defined in Appendix
B = dimensionless parameter
$\overline{B}, \overline{B}'$ = dimensionless parameters defined in Appendix
C_i = concentration of i^{th} species
D_i = average diameter of pores in i^{th} range
D_{ij} = effective binary diffusivity
D_{ij}^{at} = binary diffusivity at atmospheric pressure
D_{iK} = effective Knudsen diffusivity of i^{th} species
$D_{iK}^{\bullet}$ = Knudsen diffusivity of i^{th} species
F, F_1 = dimensionless functions
N_i = total molar flux of i^{th} species
N_i' = molar flux of i^{th} species due to diffusion
P = pressure
P_{atm} = atmospheric pressure
R = gas constant
R_p = particle diameter
T = temperature
V_i = dimensionless concentration of i^{th} species
W = dimensionless pressure

Greek Letters

β = permeability
γ_i = net molar production of i^{th} species
δ = ratio of molar productions of tar and gases
ϵ_i = porosity of i^{th} range of pores
λ_{ij} = dimensionless parameter
μ = viscosity
ρ_i = dimensionless parameter

Subscripts

I = inert carrier
G = gases
T = tar

LITERATURE CITED

Abed, R., and R. G. Rinker, "Reaction with Mole Changes in Porous Catalysts in the Molecular, Transition, and Knudsen Regimes," *AIChE J.*, **19**, 618 (1973).

Abed, R., K. Ha, and R. G. Rinker, "nth-Order Reaction with Mole Changes in Porous Catalysts in the Molecular, Transition, and Knudsen Regimes," *AIChE J.*, **20**, 391 (1974).

Anthony, D. B., J. B. Howard, H. C. Hottel, and H. P. Meissner, "Rapid Devolatilization of Pulverized Coal," *Fuel*, **55**, 121 (1976).

Arri, L. E., and N. R. Amundson, "An Analytical Study of Single Particle Char Gasification," *AIChE J.*, **24**, 72 (1978).

Balder, J. R., and E. E. Petersen, "Application of the Single Pellet Reactor for Direct Mass Transfer Studies," *J. Catalysis*, **11**, 202 (1968).

Feng, C., and W. E. Stewart, "Practical Models for Isothermal Diffusion and Flow of Gases in Porous Solids," *Ind. Eng. Chem. Fundam.*, **12**, 143 (1973).

Gavalas, G. R. and M. Oka, "Characterization of the Heavy Products of Coal Pyrolysis," *Fuel*, **57**, 285 (1978).

Jackson, R., *Transport in Porous Catalysts*, Elsevier Scientific, Amsterdam (1977).

Mason, E. A., and R. B. Evans III, "Graham's Laws: Simple Demonstrations of Gases in Motion," *J. Chem. Ed.*, **46**, 358 (1969).

Otani, W., N. Wakao, and J. M. Smith, "Effect of Pressure Gradients on the Effectiveness of Porous Catalysts," *AIChE J.*, **11**, 446 (1965).

Rao, M. R., and J. M. Smith, "Diffusion and Reaction in Porous Glass," *AIChE J.*, **10**, 293 (1964).

Russel, W. B., D. A. Saville, and M. I. Greene, "A Model for Short Residence Time Hydropyrolysis of Single Coal Particles," *AIChE J.*, **25**, 65 (1979).

Suuberg, E. M., W. A. Peters, and J. B. Howard, "Product Composition and Kinetics of Lignite Pyrolysis," *Ind. Eng. Chem. Proc. Des. Dev.*, **17**, 37 (1978).

Suuberg, E. M., "Rapid Pyrolysis and Hydropyrolysis of Coal," Ph.D. thesis, Mass. Inst. of Technology (1977).

Wakao, N., and J. M. Smith, "Diffusion in Catalyst Pellets," *Chem. Eng. Sci.*, **17**, 825 (1962).

Wakao, N., and J. M. Smith, "Diffusion and Reaction in Porous Catalysts," *Ind. Eng. Chem. Fundam.*, **3**, 123 (1964).

Wong, R. L., and V. E. Denny, "Diffusion, Flow, and Heterogeneous Reaction of Ternary Mixtures on Porous Catalytic Media," *Chem. Eng. Sci.*, **30**, 709 (1975).

APPENDIX: MASS TRANSFER IN D_4-PORES

To estimate the pressure and composition gradients in the D_4-pores, we consider the simple case of binary mass transfer (tar-gases) with $\gamma_T << \gamma_G$, which has been examined earlier. The following notational modifications and assumptions are necessary in order to use the earlier equations:

1) Replace ϵ_3, D_3 by ϵ_4, D_4.

2) Replace γ_T, γ_G by $f\gamma_T$, $f\gamma_G$. The fraction $f(0 < f < 1)$ accounts for the fact that a fraction of the products (generated on the surface of D_2 and D_3 pores) is released to the D_4-pores, and the remainder escapes to the particle surface directly. The fraction f can be estimated by

$$f = \frac{\frac{\pi D_p^3}{6} m_{34}}{\frac{\pi D_p^3}{6} m_{34} + \pi D_p^2 n_3}$$

assuming that products are transferred to the D_4-pores or directly to the particle surface via the D_3-pores (and thus neglecting the less important direct transfer from D_2-pores to D_4-pores or to the particle surface).

3) Transport in the D_4-pores will be treated by the continuum approach despite the low degree of crosslinking, in line with the approximate nature of the estimates sought.

With the above modifications, Equation (37) can be applied to the D_4-pore network to yield the maximum relative pressure

$$W(0) - 1 = \frac{1 + \overline{A}}{\overline{A}} \left\{ \left(1 + \frac{A_{at}(1 + \delta\bar{\rho}_T)\overline{B}}{(1 + \overline{A})^2} \right)^{1/2} - 1 \right\} \tag{A1}$$

where $\overline{A}$ and $\overline{B}$ are given by the expressions for A and B with the difference that transport coefficients and porosity of the D_4-pores should be used and γ_G, γ_T should be replaced by $f\gamma_G$, $f\gamma_T$. We have $\overline{A}_{at} = 10A_{at}$, still considerably less than unity. Thus, except when $\overline{B}$ is much larger than unity, (A1) can be simplified to

$$W(0) - 1 = \frac{1 + \delta\bar{\rho}_T}{2} \frac{\overline{A}_{at}}{\overline{A}(1 + \overline{A})} \overline{B} \tag{A2}$$

As before, the relative pressure increase is proportional to $\overline{B}$ and is magnified by low outside pressure and diminished by large outside pressure.

Assuming that $W(0) - 1$ is much less than unity, the mole fraction of tar in the D_4-network satisfies the simple

equation for binary bulk diffusion

$$N_T = x_T(N_T + N_G) - D_{TG}\frac{P_o}{R_gT}\frac{dx_T}{dr} \qquad (A3)$$

where the molar fluxes N_T, N_G refer to the D_4-pore network and hence are given by

$$N_i = \frac{f\gamma_i}{3}r \quad (i = G, T)$$

Introducing these expressions in (A3) and solving with the condition $x_T = 0$ at $r = R_p$, we obtain

$$x_T = \frac{\gamma_T}{\gamma_T + \gamma_G}\left\{1 - \exp\left[-\overline{B}'\left(1 - \frac{r^2}{R_p{}^2}\right)\right]\right\} \qquad (A4)$$

where

$$\overline{B}' = \frac{(1+\delta)}{2}\frac{D^{\bullet}_{GK}}{D^{at}_{TG}}\overline{B}$$

The maximum value of x_T is given by

$$x_T(0) = \frac{\gamma_T}{\gamma_T + \gamma_G}(1 - e^{-\overline{B}'}) \qquad (A5)$$

so that the criterion for small composition gradients becomes

$$\overline{B}' << 1 \qquad (A6)$$

According to (A2) the condition (A6) also insures small relative pressure gradients.

To examine the conditions under which (A6) is valid, we take the following example: $T = 800°K$, $R_p = 50\ \mu m$, $\epsilon_4 = 0.015$, weight loss = 20% in 10 s (half of which is gases and half is tar). Using molecular weights $M_G = 25$, $M_T = 250$ and coal particle density 1.2 g/cm³, we compute $\gamma_G = 4.8 \times 10^{-4}$ gmols/cm³s, $\gamma_T = 0.48 \times 10^{-4}$ gmols/cm³s, $D_{GK} = 2.74$ cm²/s, $D^{at}_{TG} = 0.48$ cm²/s, $f = 0.33$, $\delta = 0.1$ so that $\overline{B} = 0.005$, $\overline{B}' = 0.015$. On the other hand, taking $T = 900°K$ the rates are larger by a factor 3-5 so that $\overline{B}' \sim 0.04$-0.08. If, on the other hand, we take $T = 900°K$ and $R_p = 100\ \mu m$, $\overline{B} \sim 0.06$-0.11, $\overline{B}' \sim 0.16$-0.34, marking a departure from uniform conditions. Under conditions at which $\overline{B}' \lesssim 1$, the use of an effective radius as defined by Equation (5) underestimates the internal build-up of pyrolysis products.

Manuscript received August 3, 1978; revision received April 23, and accepted August 20, 1979.

Thermodynamics of Microemulsions: Combined Effects of Dispersion Entropy of Drops and Bending Energy of Surfactant Films

C. A. MILLER

and

P. NEOGI

Department of Chemical Engineering
Carnegie-Mellon University
Pittsburgh, Pennsylvania 15213

A theory of dilute microemulsions is presented which includes for the first time both the entropy of dispersion of the drops and energy effects associated with bending the surfactant films at the drop interfaces. It yields expressions for drop size for (a) a dilute microemulsion in equilibrium with an excess bulk phase, e.g., an oil-in-water microemulsion in equilibrium with excess oil and (b) dilute oil-continuous and water-continuous microemulsions in equilibrium and containing equal amounts of surfactant. In the latter case, our theory indicates that existence of the two microemulsion phases sometimes is favored over a layered or lamellar phase, even though the "natural curvature" of the surfactant films is zero, corresponding to a perfectly flat film.

SCOPE

"Microemulsions are dispersions of one liquid in another which have very small drops (< 0.1 μm) and are often thermodynamically stable. They have been used in such applications as cutting oils and pesticides and are currently of great interest in connection with processes for increasing recovery of petroleum from underground reservoirs.

An important property of a microemulsion is its drop size. Existing theory indicates that drop size has a large effect on the interfacial tensions a microemulsion makes with other phases it contacts. Interfacial tension, in turn, has a strong influence on process success for the petroleum recovery situation. Thus, a theory which could predict drop size in microemulsions would be of considerable interest.

Other researchers have shown that both the entropy of dispersion of the many small drops and the energy required to bend the surfactant films at the drop interfaces are important in determining drop size in microemulsions. But no existing theory includes both effects. Such a theory is presented here.

P. Neogi is presently at the State University of New York, Buffalo, New York 14214.

0001-1541-80-2177-0212-$01.05.